Journal of Neuroscience Methods 223 (2014) 133–143

Contents lists available at ScienceDirect

Journal of Neuroscience Methods

journal homepage: www.elsevier.com/locate/jneumeth

Generation of a neurodegenerative disease mouse model using lentiviral vectors carrying an enhanced synapsin I promoter

Yasunori Matsuzaki, Miho Oue, Hirokazu Hirai*

Department of Neurophysiology, Gunma University Graduate School of Medicine, Maebashi, Gunma 371-8511, Japan

HIGHLIGHTS

- We developed a new hybrid promoter having high neuronal specificity.
- The promoter showed efficient and specific neuronal transduction in the cerebellum.
- Spinocerebellar ataxia model mice were lentivirally generated using the promoter.
- The model mice showed neuron-specific transgene expression throughout the CNS.
- The model mice showed ataxia and neuronal inclusions characteristic to the disease.

ARTICLE INFO

Article history:
Received 11 July 2013
Received in revised form
26 November 2013
Accepted 5 December 2013

Keywords:
Synapsin I promoter
Cerebellum
Lentiviral vector
Transgenic mouse
Spinocerebellar ataxia
Ataxin-1

ABSTRACT

Background: Certain inherited progressive neurodegenerative disorders, such as spinocerebellar ataxia (SCA), affect neurons in large areas of the central nervous system (CNS). The selective expression of disease-causing and therapeutic genes in susceptible regions and cell types is critical for the generation of animal models and development of gene therapies for these diseases. Previous studies have demonstrated the advantages of the short synapsin I (SynI) promoter (0.5 kb) as a neuron-specific promoter for robust transgene expression. However, the short SynI promoter has also shown some promoter activity in glia and a lack of transgene expression in significant areas of the CNS.

New methods: To improve the SynI promoter, we used a SynI promoter that is twice as long (1.0 kb) as the short SynI promoter and incorporated a minimal CMV (minCMV) sequence.

Results: We observed that the 1.0 kb rat SynI promoter with minCMV [rSynI(1.0)-minCMV] exhibited robust promoter strength, excellent neuronal specificity and wide-ranging transgene expression throughout the CNS.

Comparison with existing methods: Compared with the two previously reported short (0.5 kb) promoters, the new promoter was superior with respect to neuronal specificity and more efficiently transduced neurons. Moreover, transgenic mice expressing the mutant protein ATXN1[Q98], which causes SCA type 1 (SCA1), under the control of the rSynI(1.0)-minCMV promoter showed robust transgene expression specifically in neurons throughout the CNS and exhibited progressive ataxia.

Conclusion: rSynI(1.0)-minCMV drives robust and neuron-specific transgene expression throughout the CNS and is therefore useful for viral vector-mediated neuron-specific gene delivery and generation of neuron-specific transgenic animals.

1. Introduction

Previous studies comparing several neuron-specific promoters have shown that the synapsin I (SynI) promoter is superior in terms of promoter strength and neuronal specificity (Boulos et al., 2006; Hioki et al., 2007; Kugler et al., 2003; Nakagawa et al., 2006). Because the SynI promoter is phylogenetically well conserved, promoters from rats and humans are often used for the generation of neuron-specific transgenic mice (Guo et al., 2002; Heumann et al., 2000; Hoesche et al., 1993; Holzer et al., 2001; Morimoto et al., 2002; Nakagawa et al., 2006; Sargeant et al., 2012; Scott and Lois, 2005) or viral vector-mediated gene transfer into rodent neurons (Dittgen et al., 2004; Hioki et al., 2007; Kugler et al., 2003). The first transgenic mice expressing a transgene under control of the SynI promoter carried a construct containing ~4300 nucleotides of the 5′-flanking sequence of the rat synapsin gene (Hoesche et al., 1993). The size of the SynI promoter in these transgenic mice was gradually shortened in subsequent

* Corresponding author. Tel.: +81 27 220 7930; fax: +81 27 220 7936.
E-mail address: hirai@gunma-u.ac.jp (H. Hirai).

0165-0270/$ – see front matter © 2013 Elsevier B.V. All rights reserved.
http://dx.doi.org/10.1016/j.jneumeth.2013.12.004

studies (Heumann et al., 2000; Morimoto et al., 2002; Nakagawa et al., 2006; Sargeant et al., 2012; Scott and Lois, 2005). However, recent studies using shorter versions of the SynI promoter have failed to demonstrate robust transgene expression in the hindbrain. For example, Nakagawa et al. (2006) generated transgenic mice expressing glutamate receptor interacting protein 1 (GRIP1), a postsynaptic protein, under the control of a 450-bp human SynI promoter; however, these mice did not show transgene expression in the cerebellum, although transgene expression was observed in the brainstem, olfactory bulb, forebrain and hippocampus. More recently, transgenic mice carrying a 585-bp human SynI promoter showed minimal expression of the transgene in several regions, including the brainstem and spinal cord, in contrast to the abundant expression observed in the cerebrum and hippocampus (Sargeant et al., 2012). These results suggest that the deleted region might be required for stable transgene expression throughout the central nervous system (CNS).

A major disadvantage of cell type-specific promoters is their weaker transcriptional activity when compared with constitutive viral promoters such as the cytomegalovirus (CMV) promoter and the murine stem cell virus (MSCV) promoter (Boulos et al., 2006; Nakagawa et al., 2006). Hioki et al. (2007) increased transcriptional activity 2-to-3-fold after fusing the CMV enhancer to the human SynI promoter (401 bp), as verified through the lentiviral expression of GFP in the rat neostriatum, thalamus and neocortex *in vivo*. However, the addition of the CMV enhancer significantly decreased the neuronal specificity of neuron-specific promoters, including the SynI promoter (Hioki et al., 2007). These results suggest that addition of the CMV enhancer is beneficial for increasing transcriptional activity but might potentially compromise neuronal specificity.

Spinocerebellar ataxias (SCAs) are progressive neurodegenerative diseases of multiple types. SCAs impair a wide range of CNS regions, including the cerebral cortex, thalamus, midbrain, cerebellum, brainstem and spinal cord (Seidel et al., 2012). Neuronal nuclear inclusions are a hallmark of many types of SCAs, such as SCA type 1, type 3 and type 7 (Seidel et al., 2012), indicating that neurons are the primary cell types affected by these SCA types. The selective delivery of disease-causing genes to susceptible regions and cell types is critical for the generation of animal models. Although many different types of SCA mouse models have been genetically engineered, there are no SCA mouse models showing diffuse expression of disease-causing genes exclusively in neurons in the CNS (Ingram et al., 2012). Although the SynI promoter is an ideal candidate for the generation of these animals, previous studies using short SynI promoters have found either no transgene expression or scarce expression in the cerebellum and brainstem (Nakagawa et al., 2006; Sargeant et al., 2012). The aim of the present study was to obtain a SynI promoter with high neuronal specificity and robust transcriptional activity extensively in the CNS. The behavior of the SynI promoter in the cerebellum has not been extensively studied; thus, using lentiviral vectors, we initially examined the transduction profile of three different SynI promoters of different lengths carrying CMV-derived enhancers in the cerebellums of mice. As a result, we generated an SCA mouse model using 1.0 kb of the rat SynI promoter fused with the minimal CMV promoter (minCMV) sequence.

2. Materials and methods

2.1. Animals

C57BL/6J (BL6) mice were purchased from CLEA (Tokyo, Japan), and ICR mice were obtained from Charles River Laboratories (Kanagawa, Japan) and Japan SLC (Sizuoka, Japan). Nine BL6 mice and 23 ICR mice were used in this study. All procedures for the care and treatment of animals were performed according to the Japanese Act on the Welfare and Management of Animals and the Guidelines for the Proper Conduct of Animal Experiments issued through the Science Council of Japan. The experimental protocol was approved through the Institutional Committee of Gunma University (no. 09-062). All efforts were made to minimize suffering and reduce the number of animals used.

2.2. Construction of modified SynI promoters

For the construction of rSynI(1.0)-minCMV (Fig. 1A and B), 1.0 kb of the rat SynI promoter region (nucleotides 1–1046; GenBank: DD464830.1) was amplified by polymerase chain reaction (PCR) of rat genomic DNA (1st PCR in Supplementary Fig. 1A). The minCMV sequence (nucleotides 1091–1218; GenBank: X03922.1) was amplified by PCR of the CMV IE1 promoter (1st PCR in Supplementary Fig. 1A). The 5′ end of the forward primer for the minCMV fragment amplification contained a sequence overlapping the 3′ end of the rat SynI promoter; thus, the rat SynI promoter and minCMV fragments were directly combined through overlapping PCR (Overlapping 2nd PCR in Supplementary Fig. 1A). rSynI(0.5)-minCMV (containing nucleotides 511–1046; GenBank: DD464830.1) was obtained from rSynI(1.0)-minCMV by the 3rd PCR depicted in Supplementary Fig. 1A.

CMVe-hSynI(0.4) was constructed as previously reported (Hioki et al., 2007). Briefly, using PCR, the CMV enhancer (CMVe, nucleotides 1–364; GenBank: X03922.1) and 0.4 kb of the human synapsin I promoter region (hSynI, nucleotides 1889–2289; GenBank: M55301.1) were amplified from the CMV promoter and human genome, respectively, and the two PCR products were ligated after restriction enzyme (PstI) digestion (Supplementary Fig. 1B). The sequences of all primers used for generation of the three hybrid promoter constructs are shown in Supplementary Fig. 1C.

The generated promoters were inserted into the MluI/EcoRI-digested site of the pCL20c-GFP lentiviral vector plasmid provided by St. Jude Children's Research Hospital (Memphis, TN, USA) (Fig. 1A and B).

2.3. Construction of a lentiviral vector plasmid expressing ATXN1[Q98]

P2A, a 'self-cleaving' peptide sequence (ATNFSLLKQAGDVEENPGP), was inserted between GFP and HA-ATXN1[Q98], which freed GFP from HA-ATXN1[Q98] by ribosomal skipping between glycine and proline (Donnelly et al., 2001; Iizuka et al., 2009; Kuzmich et al., 2013). The woodchuck hepatitis virus posttranscriptional regulatory element (WPRE) sequence was inserted following ATXN1[Q98] at the ClaI-digested site of pCL20c (Donello et al., 1998; Zufferey et al., 1999).

The human ataxin-1 gene was amplified using reverse transcription PCR, and the human influenza hemagglutinin (HA) tag sequence was attached to the 5′ end of the ataxin-1 gene. To enhance the pathology when expressed in transgenic mice, the number of CAG repeats in the ataxin-1 gene was expanded to 98 repeats using two-step PCR (Laccone et al., 1999). Briefly, two ataxin-1 fragments from the 5′ end to the CAG repeat region and from the CAG repeat region to the 3′ end were produced through PCR using two pairs of primers: ATXN1-F (forward primer), 5′-CGACGCGTGCCACCATGTACCCATACGAT-3′/CTG7-R (reverse primer) 5′-CTGCTGCTGCTGCTGCTGCTG-3′ and CAG7-F (forward primer), 5′-CAGCAGCAGCAGCAGCAGCAG-3′/ATXN1-R (reverse primer), 5′-CCATCGATCTACTTGCCTACATTAGACC-3′. The 5′- and 3′-end fragments obtained from the 1st PCR reaction were mixed together after gel purification, and a 2nd PCR reaction was performed using ATXN1-F (a forward primer) and ATXN1-R (a reverse primer) to obtain the full-length ataxin-1 gene. The conditions used for the 1st and 2nd PCR reactions were 40 cycles of 98 °C for

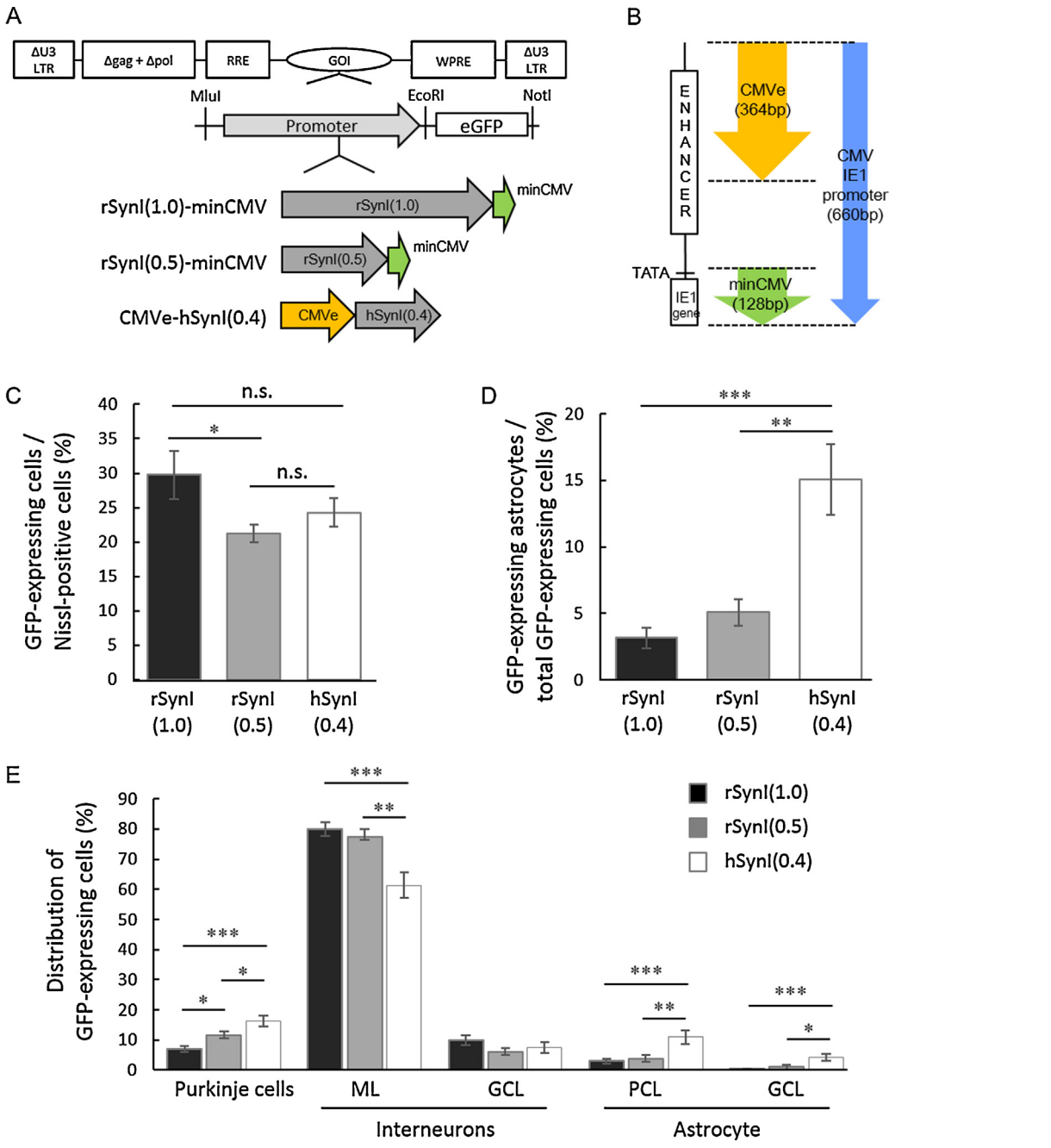

Fig. 1. Comparison of three altered human or rat synapsin I (SynI) promoters of different sizes. (A) Schema depicting the proviral region flanked by U3-deleted long terminal repeats (ΔU3LTRs) and the composition of three modified SynI promoters. Each of the modified SynI promoters and the enhanced green fluorescent protein (GFP) gene were inserted into lentiviral vectors as the GOI (gene of interest) and positioned upstream of the woodchuck hepatitis virus posttranscriptional regulatory element (WPRE). The three promoters include the human SynI promoter (0.4 kb) and two rat SynI promoters (0.5 kb and 1.0 kb). The human and rat SynI promoters were fused with the 364-bp cytomegalovirus (CMV) enhancer (CMVe, yellow arrow) at the 5′ end [CMVe-hSynI(0.4)] or with a 128-bp minimal CMV (minCMV, green arrow) at the 3′ end [rSynI(1.0)-minCMV and rSynI(0.5)-minCMV], respectively. Δgag, deleted gag sequence; Δpol, deleted pol sequence; RRE, rev response element. (B) A diagram showing the components of the CMV IE1 promoter and the relative positions of CMVe and minCMV in the CMV IE1 promoter (blue arrow). The CMV IE1 promoter includes the enhancer region (ENHANCER), TATA box and immediate early 1 (IE1) gene. (C) Percentage of neurons transduced by lentiviral vectors containing one of the modified SynI promoters. Three mice were used for the analysis of each promoter (a total of nine mice for three promoters). We counted the number of GFP-expressing cells in more than 2000 Nissl-positive neurons in lobule 4/5 from three mice, and the percentage ratios are expressed in the graph. (D) Decrease in the neuronal specificity of three modified SynI promoters. Three mice were used for the analysis of each promoter. We counted the number of S-100-positive astrocytes in more than 500 GFP-expressing-cells in lobule 4/5, and the percentage ratio is expressed in the graph. (E) Cell types transduced by the modified rat or human SynI promoters. Three mice received an injection of a lentiviral vector containing one of the modified SynI promoters (a total of nine mice for three promoters). Cerebellar sections were labeled for S-100 and Nissl. The number of Purkinje cells, interneurons and astrocytes in more than 500 GFP-positive cells in lobule 4/5 from three mice were counted, and their ratios were determined. Purkinje cells were distinguished from interneurons by their unique morphology and diameter of the soma. ML, molecular layer; GCL, granule cell layer; PCL, Purkinje cell layer. The data are the means ± S.E.M. Statistical analysis was performed by one-way ANOVA with Tukey's post hoc test: * $p < 0.05$, ** $p < 0.01$, *** $p < 0.001$. n.s., not significant. (For interpretation of the references to color in this figure legend, the reader is referred to the web version of this article.)

10 s, 60 °C for 5 s and 72 °C for 90 s. After expansion of the CAG tract, the ataxin-1 gene was inserted into the NotI restriction site of the pCL20c-rSynI(1.0)-minCMV-GFP-P2A-(NotI)-WPRE plasmid using KOD-Plus-NEO polymerase (Toyobo, Osaka, Japan) and the InFusion HD cloning kit (Takara Bio, Shiga, Japan) (Fig. 4A).

2.4. Production and titration of lentiviral vectors

The vesicular stomatitis virus-glycoprotein (VSV-G)-pseudotyped lentiviral vector was produced in HEK293T cells (Thermo Fisher Scientific, Kanagawa, Japan), as previously described (Torashima et al., 2008). The plasmids were transfected into HEK293T cells using the calcium phosphate method. After 48 h, the supernatant, containing viral particles, was harvested, ultracentrifuged (CP80WX; Hitachi Koki, Tokyo, Japan) and resuspended in 70 μl of Dulbecco's phosphate-buffered saline (−). The resultant lentiviral solution was stored at 4 °C and used within 3 weeks. The viral titers were measured using the quantitative real-time RT-PCR method. We used an RNeasy Mini Kit (Qiagen, Tokyo, Japan) to prepare genomic RNA from 1 μl of the viral solution. Reverse transcription was performed using the ReverTra Ace qPCR RT Master Mix with gDNA Remover (Toyobo). For viral titration, quantitative real-time PCR was performed using the Takara thermal cycler Dice TP800 system (Takara Bio) and SYBR Premix Ex Taq II (Takara Bio) with cycles at 95 °C for 5 s and 60 °C for 30 s. The following primer pairs were used: EGFP-F, 5′-CGACCACTACCAGCAGAACAC-3′ and EGFP-R, 5′-TGTGATCGCGCTTCTCGTTGG-3′.

2.5. Generation of transgenic mice

Transgenic mice were generated after lentiviral injection into the perivitelline space of 2-cell mouse embryos, as previously described (Oue et al., 2012). The 2-cell embryos collected from superovulated ICR female mice were treated with serotropin (5IU; ASKA Pharmaceutical Co., Tokyo, Japan) and gonatropin (5IU; ASKA Pharmaceutical Co.). The lentiviral microinjection was performed using a FemtoJet microinjector (Eppendorf AG, Hamburg, Germany) equipped with a FemtoTip (Eppendorf AG) and a three-axis hanging joystick oil hydraulic micromanipulator (Narishige, Tokyo, Japan). The injected embryos were transplanted into the oviducts of pseudo-pregnant females. Fluorescent images of the brain and spinal cord of newborn pups were obtained using a CCD camera (VB-7010; Keyence, Osaka, Japan) attached to a fluorescence stereoscopic microscope (VB-L10; Keyence). The genotyping was performed by PCR amplification of genomic DNA samples from the toe tips of weaned pups using the following primers: minCMV-F, 5′-TTTTGACCTCCATAGAAGACACC-3′ and EGFP-R, 5′-TGGTGCAGATGAACTTCAGGG-3′.

2.6. Histological analysis

The mice were deeply anesthetized with a combination of ketamine (150 mg/kg body weight) and xylazine (15 mg/kg body weight) and transcardially perfused with PBS and a fixative containing 4% paraformaldehyde in 0.1 M phosphate buffer. The brains were cut into 50 μm sagittal sections using a microslicer (DTK-1000; Dosaka, Kyoto, Japan). Images of GFP fluorescence were obtained using a fluorescence microscope (BZ-9000; Keyence) or a confocal laser-scanning microscope (LSM 5 PASCAL; Carl Zeiss, Oberkochen, Germany).

2.7. Immunohistochemistry

Floating brain sections were immunostained in blocking solution (2% bovine serum albumin, 2% normal donkey serum and 0.4% Triton X-100 in phosphate buffer) for 1 day at 4 °C with the following primary antibodies: rat monoclonal anti-GFP (1:1000; 04404-84; Nacalai Tesque, Kyoto, Japan), rabbit monoclonal anti-GFP (1:1000; GFP-Rb-Af2020-1; Frontier Institute, Hokkaido, Japan), mouse monoclonal anti-S100 (1:1000; S2532; Sigma-Aldrich, St. Louis, MO, USA), rat monoclonal anti-HA (1:1000; 1867423; Roche Diagnostics, Basel, Switzerland) and rabbit polyclonal anti-calbindin D-28K (1:500; AB1778; Merck Millipore, Billerica, MA). The bound primary antibodies were visualized after incubation with Alexa Fluor 488 donkey anti-rat IgG (1:1000; Life Technologies, Gaithersburg, MD, USA), Alexa Fluor 568 donkey anti-mouse IgG (1:1000; Life Technologies) and Alexa Fluor 568 donkey anti-rat IgG (1:1000; Life Technologies) in blocking solution for 2 h at room temperature. After the secondary antibody reaction, Nissl bodies were stained using NeuroTrace 530/615 (1:200; Life Technologies) or NeuroTrace 640/660 (1:200; Life Technologies) in PBS for 40 min at room temperature.

2.8. Measurement of the thickness of the molecular layer in the cerebellar cortex

The thicknesses of the molecular layers from 3 SCA1 model founders (no. 66, no. 68 and no. 69) were measured and compared with that of wild-type mice. Because the SCA1 model founder no. 68 was sacrificed at 26 weeks of age, three wild-type mice at 26 ± 2 weeks of age were used for comparison, while 34–38-week-old wild-type mice were used as controls for the SCA1 model founders no. 66 and no. 69, which were sacrificed at 38 weeks of age. Sagittal sections (50 μm thickness) were prepared from the cerebellar vermis (within 0.4 mm from the midline) and immunolabeled for calbindin-D28K. Immunofluorescence images of the cerebellar cortex were obtained with a confocal laser-scanning microscope (LSM 5 PASCAL, Carl Zeiss). The thickness of the molecular layer was measured at lobule 3, lobule 6 and lobule 9 using two cerebellar sections from one mouse. The exact locations at which the thickness was measured are depicted in Fig. 7A. The molecular layer was defined from the origin of the primary dendrites of Purkinje cells to the distal end just below the pia mater.

3. Results

3.1. Assessment of the promoter strength and neuronal specificity of the three SynI promoters

We prepared three SynI promoters of different lengths fused with CMV-derived enhancers (Fig. 1A). One promoter, comprising the 401-bp human SynI promoter with the upstream 364-bp CMVe from the CMV E1 promoter [CMVe-hSynI(0.4)] (Fig. 1B), has been previously reported as being superior to other neuron-specific promoters in terms of neuronal specificity and transcriptional activity (Hioki et al., 2007). The other two promoters comprised 0.5 or 1.0-kb rat SynI promoters with a downstream minCMV region from the CMV E1 promoter [rSynI(0.5)-minCMV or rSynI(1.0)-minCMV, respectively] (Fig. 1A and B). Each of the promoters, together with the enhanced green fluorescent protein (GFP) gene, was subcloned into the lentiviral plasmid (Fig. 1A). The WPRE was placed downstream of the GFP gene to enhance gene expression (Donello et al., 1998; Zufferey et al., 1999).

The promoter strength and neuronal specificity of the modified SynI promoters were examined through the lentiviral vector-mediated expression of GFP in the cerebellar cortex. After adjusting the genome titers of the lentiviral vectors, 10 μl of lentiviral solution was injected into the subarachnoidal space over lobules 4/5 of the cerebella of 3 C57BL/6 mice at postnatal day (P) 21–24. The mice were examined at 7 days after viral injection. Fluorescent

stereoscopic examination showed bright fluorescence in the cerebella treated with lentiviral vectors expressing GFP under the control of the modified SynI promoter (Supplementary Fig. 2A–C). To assess the transduction area and cell types in the cerebellum, sagittal slices were immunostained for Nissl substance, a neuronal marker, or S-100, an astrocyte marker. Low-magnification images of the sagittal sections of the cerebellum showed a fairly similar range of GFP expression, which was centered at lobules 4/5 and extended to the cortex of lobule 9 through the white matter (Supplementary Fig. 2D–F). These results suggest that rSynI(0.5)-minCMV and rSynI(1.0)-minCMV exhibit strong transcriptional activity similar to CMVe-hSynI(0.4), which was previously reported to have strong promoter activity (Hioki et al., 2007). The enlarged images around lobules 4/5 showed that all three promoters induced GFP expression primarily in neurons, which were morphologically distinguished as Purkinje cells and interneurons such as stellate, basket and Golgi cells (Supplementary Fig. 2G–I). As reported previously (Torashima et al., 2006), the lentiviral vectors did not transduce granule cells. To quantitate the efficiency of lentiviral transduction of neurons, we counted neurons that were double-positive for GFP and Nissl in the cortex of lobule 4/5 and divided this number by the number of Nissl-positive cells, omitting granule cells because no granule cells were transduced by lentiviral vectors. rSynI(1.0)-minCMV caused a significantly higher neuronal transduction frequency (29.7%) than rSynI(0.5)-minCMV (21.3%) (Fig. 1C).

Some GFP-expressing cells were immunolabeled for S-100, a glial marker, which revealed that the modified SynI promoters were not 100% specific for neurons (Supplementary Fig. 2J–L, arrowheads). To assess the neuronal specificity of the three promoters, we determined the ratio of astrocytes that were double-positive for GFP and S-100 to the total number of GFP-positive cells in lobule 4/5 (Fig. 1C). CMVe-hSynI(0.4) showed significantly greater expression in astrocytes (15.1%) than did 1.0 kb and 0.5 kb rat synapsin I-based promoters (3.1% and 5.1%, respectively) (Fig. 1D).

We next examined the cortical cell types transduced by the three promoters. We analyzed more than 500 GFP-expressing cells in the cerebellar cortices from three mice that were treated with lentiviral vectors containing one of the modified SynI promoters, and the percent ratio of Purkinje cells, interneurons and astrocytes to total GFP-expressing cells was calculated (Fig. 1E). Consistent with the results shown in Fig. 2D, the astrocyte ratio was significantly higher in cells transduced with CMVe-hSynI(0.4) (15.1%) compared with those transduced with the two other modified rat SynI promoters (3–5%). CMVe-hSynI was more likely to transduce Purkinje cells (16.1%) than the modified rat SynI promoters (7.0–11.7%); however, the modified rat SynI promoters transduced interneurons in the molecular layer (namely, stellate cells and basket cells) significantly more efficiently than CMVe-hSynI.

We further examined the transduction profiles of the three promoters on the basis of GFP intensity in Purkinje cells, interneurons and astrocytes, which was measured in the somata of

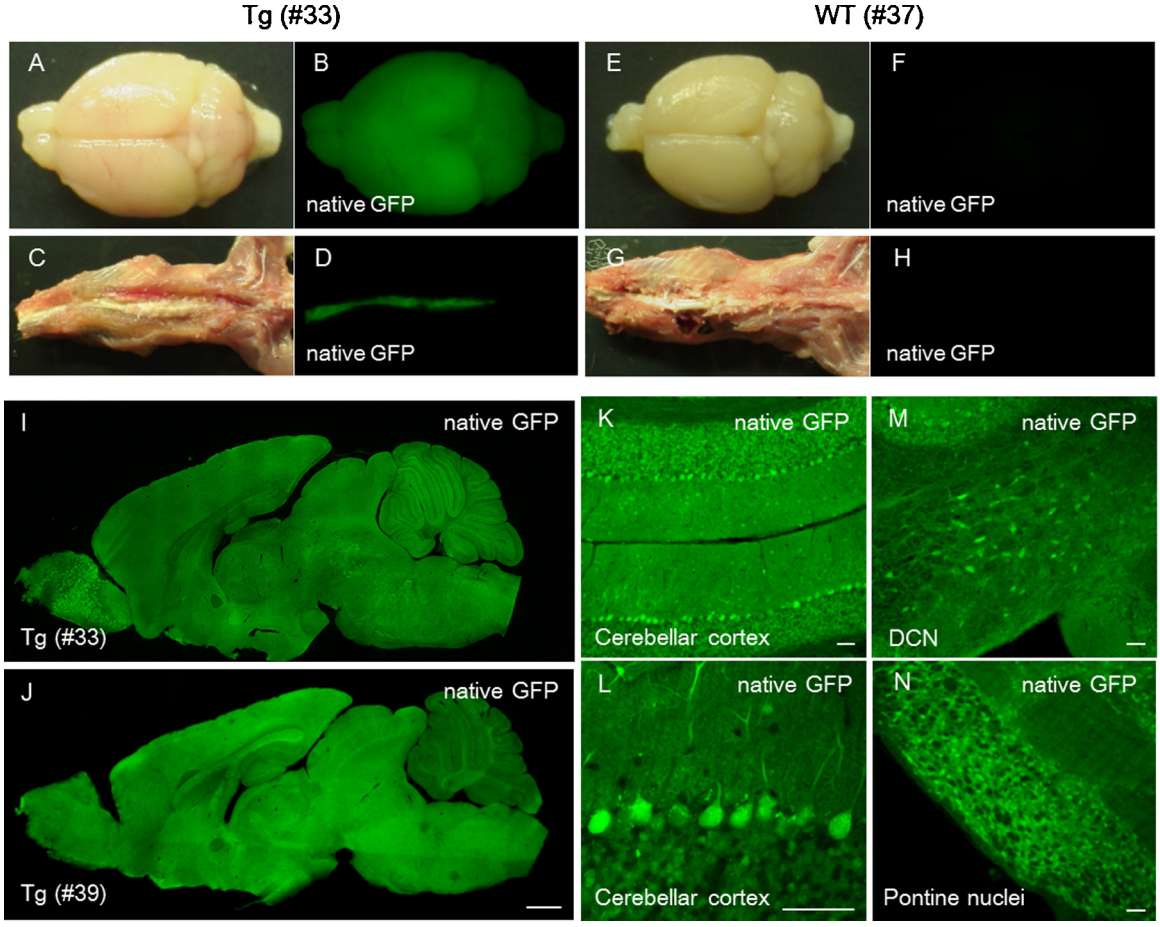

Fig. 2. Lentiviral-generated transgenic mice expressing GFP under the control of rSynI(1.0)-minCMV in the CNS. (A–H) Native GFP fluorescence and bright field (BF) images of the brain and spinal cord from a P35 transgenic mouse (no. 33) (A–D) and an age-matched wild-type littermate (E–H). (I and J) GFP fluorescence images of sagittal sections of whole brains from a transgenic mouse (no. 33, P35) and transgenic littermate (no. 39, P378). (K–N) Native GFP fluorescence images of the cerebellar cortex (K and L), deep cerebellar nuclei (DCN) (M) and pontine nuclei (N) from a transgenic mouse (no. 39). An enlarged image of the cerebellar cortex (L) shows the efficient expression of GFP in Purkinje and granule cells. Scale bars = 1 mm (J) and 50 μm (K–N).

GFP-expressing cells using ImageJ. GFP intensity in Purkinje cells transduced by lentiviral vectors containing rSynI(1.0)-minCMV was significantly lower than that in cells transduced with the other two promoters (Supplementary Fig. 3). On the other hand, the GFP intensity in interneurons of the granule cell layer transduced by lentiviral vectors containing CMVe-hSynI(0.4) was approximately half that observed in cells transduced by lentiviral vectors containing the modified rat SynI promoters. Taken together, these data indicate that rSynI-minCMV is superior to CMVe-hSynI(0.4) in terms of neuronal specificity, and rSynI(1.0)-minCMV significantly more efficiently transduced cerebellar cortical neurons compared with rSynI(0.5)-minCMV. Thus, it seemed that rSynI(1.0)-minCMV was superior to the other two promoters for efficient and specific neuronal transduction.

3.2. Generation of transgenic mice that express GFP under the control of rSynI(1.0)-minCMV

To examine the transgene expression profile of the rSynI(1.0)-minCMV in the CNS, transgenic mice expressing GFP under the control of the rSynI(1.0)-minCMV promoter were produced through the lentiviral vector-mediated transfer of the transgene into the chromosomes of fertilized eggs. In total, 8 of the 13 pups generated possessed the transgene. The brain (Supplementary Fig. 4A and B, arrows) and spinal cord (Supplementary Fig. 4A and B, arrowheads) of the live transgenic pups emitted bright fluorescence that was visible through the bones and skin under fluorescent stereoscopic microscopy. The transgenic mice, together with their wild-type littermates, were sacrificed at P35 (no. 33) and P378 (no. 39). Examination of transgenic mouse no. 33 revealed robust GFP expression throughout the CNS under fluorescent stereotaxic microscopy (Fig. 2A–D). The observed signal was not autofluorescence because almost no fluorescent signal was observed in the brain and spinal cord of an age-matched wild-type mouse (Fig. 2E–H). The sagittal sections of the brain from two transgenic mice (Fig. 2I and J) showed bright GFP fluorescence throughout the brains, even at 1 year after birth (no. 39, Fig. 2J). Although the expression of GFP in the cerebellum was lower than that in the other brain regions in transgenic mouse no. 39 (Fig. 2J), the enlarged images of the cerebellum and associated brainstem regions showed abundant GFP expression in Purkinje and granule cells as well as in neurons in the deep cerebellar and pontine nuclei (Fig. 2K–N).

To confirm neuron-specific GFP expression, brain sections were immunostained for Nissl substance. GFP was expressed extensively in most neurons in the cerebellum and associated brainstem nuclei, such as pontine, vestibular and inferior olivary nuclei (Fig. 3). Similar levels of GFP were detected in neurons elsewhere in the brain, including the cerebral cortex, hippocampus, thalamus and basal ganglia (data not shown). Quantitative analysis of the transgenic mice (no. 33 and no. 39) revealed that more than 99.5% of GFP-expressing cells were neurons (Table 1).

3.3. Generation of SCA1 model mice expressing mutant ataxin-1 and GFP via rSynI(1.0)-minCMV

We next examined whether rSynI(1.0)-minCMV could be used for the generation of a mouse model of disease that affects neurons diffusely in the CNS. In this study, we selected SCA type 1 (SCA1), which impairs the cerebral cortex, basal ganglia, thalamus, hippocampus, brainstem and cerebellum (Seidel et al., 2012). SCA1 was induced through the abnormal expansion of CAG repeats in the *sca1* gene (Orr et al., 1993), leading to the production of ataxin-1 protein (ATXN1) with an abnormally expanded polyglutamine tract. Mutant ATXN1 forms nuclear aggregates with nuclear proteins that are critical for neuronal function, resulting in neurodegeneration and cell death. Using lentiviral vectors, we generated

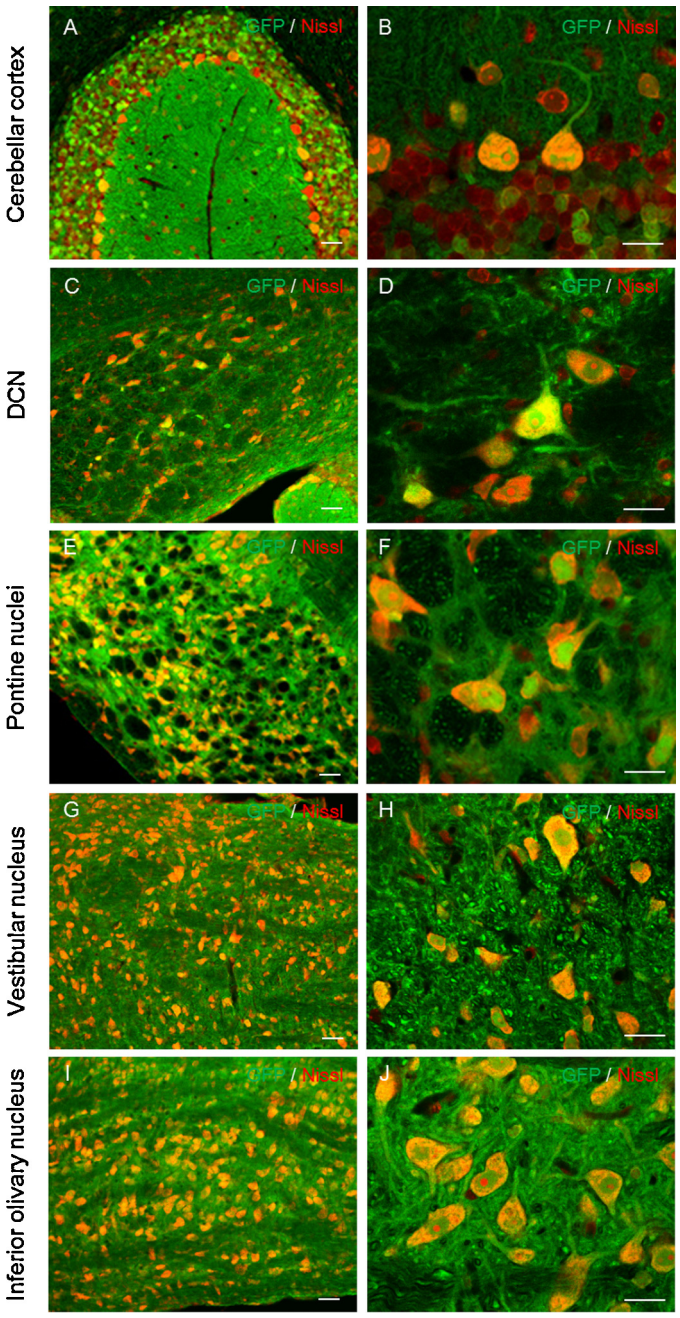

Fig. 3. Neuron-specific transgene expression in transgenic mice expressing GFP under the control of rSynI(1.0)-minCMV. Sagittal brain sections were double-immunolabeled for Nissl substance (red) and GFP (green). The images on the right are magnifications of the images shown on the left. (A and B) Cerebellar cortex; (C and D) deep cerebellar nuclei (DCN); (E and F) pontine nuclei; (G and H) vestibular nucleus; (I and J) Inferior olivary nucleus. Scale bar = 20 μm. (For interpretation of the references to color in this figure legend, the reader is referred to the web version of this article.)

transgenic mice expressing GFP and ATXN1 containing a stretch of 98 polyglutamine residues (ATXN1[Q98]) under the control of rSynI(1.0)-minCMV (Fig. 4A).

The 17 embryos that received lentiviral injections were returned to a pseudo-pregnant female mouse. Six pups (no. 66–71) were obtained, all of which were genotype positive. The brains and spinal cords of the P3 pups emitted bright fluorescence that was visible through the bones and skin under fluorescent stereoscopic microscopy (Fig. 4B and C). The SCA1 model mice gained body weight steadily with increasing growth. However, no. 68 started

Table 1
Neuronal specificity of the transgenic mice generated in the current study that express transgenes via the rSynI(1.0)-minCMV promoter. Nissl was labeled in neurons with NeuroTrace. The percent ratios of neurons among the GFP-expressing cells were determined in the various brain regions. In each region, 200–450 GFP-expressing cells were examined. DCN, deep cerebellar nuclei.

	GFP		GFP-P2A-ATXN1(Q98)		
	No. 33	No. 39	No. 66	No. 68	No. 69
Cerebellar cortex	99.5	100	98.8	100	99.3
DCN	100	100	100	100	100
Pontine nuclei	99.6	99.6	100	100	99.7
Hippocumpus	100	100	100	100	100
Cerebral cortex	99.7	99.6	99.7	100	100
Total	99.8	99.9	99.7	100	99.8

Percent ratio of GFP- and Nissl-double-positive-cells in generated transgenic mice.

to lose weight at 20 weeks of age (Fig. 4D). The other two mice (no. 66 and no. 69) also started to lose weight gradually beginning at 27 weeks. Consistently, the three mice showed clasping (Supplementary Fig. 5A) and ataxic behavior (Supplementary Fig. 5B and Supplementary movie). Ataxia became more severe with time; thus, the three mice were euthanized at 26 (no. 68) and 38 (no. 66 and no. 69) weeks of age. Transgenic mouse no. 71 died spontaneously at 49 weeks of age.

The whole brains and spinal cords from the SCA1 model mice (no. 68, no. 66 and no. 69) emitted bright GFP fluorescence under fluorescent stereoscopic microscopy (Fig. 5A and B and Supplementary Fig. 6A–D). Sagittal sections showed diffuse GFP expression throughout the brain (Fig. 5C and Supplementary Fig. 6E and F). Enlarged images of a sagittal section from mouse no. 68 showed efficient GFP expression in Purkinje and granule cells in the cerebellar cortex (Fig. 5D) as well as cells in the deep cerebellar, pontine (data not shown) and inferior olivary nuclei (Fig. 5E). The disrupted arrangement of Purkinje cell somata was clearly visible (Fig. 5D).

We next examined neuronal specificity in the transgenic mice by measuring the ratio of neurons (cells double-positive for GFP and Nissl) in transduced cells (GFP-positive cells) in the cerebellar cortex, deep cerebellar nuclei, pontine nuclei, CA3 of the hippocampus and cerebral cortex. We counted 200–450 GFP-positive cells in each region from each mouse. The result showed that the neuronal specificity was greater than 99.3% in all regions of the transgenic mice examined (Table 1).

To visualize the expression and localization of ATXN1[Q98], we immunostained brain sections from the SCA1 model mice and a control wild-type mouse (28 weeks old) for HA, which was *N*-terminally fused with ATXN1[Q98], and Nissl substance (Fig. 6). The mice used for immunohistochemistry were relatively older (26- and 38-week-old) mice; therefore, non-specific granular immunolabeling of lipofuscin was observed in the cytoplasm but not in the nuclei (Brunk and Terman, 2002; Nandy, 1971). In addition to the non-specific immunolabeling, all 3 SCA1 mouse models (no. 68, no. 66 and no. 69) showed ATXN1[Q98] aggregates localized diffusely in the nuclei of neurons in the cerebellar cortex, deep cerebellar

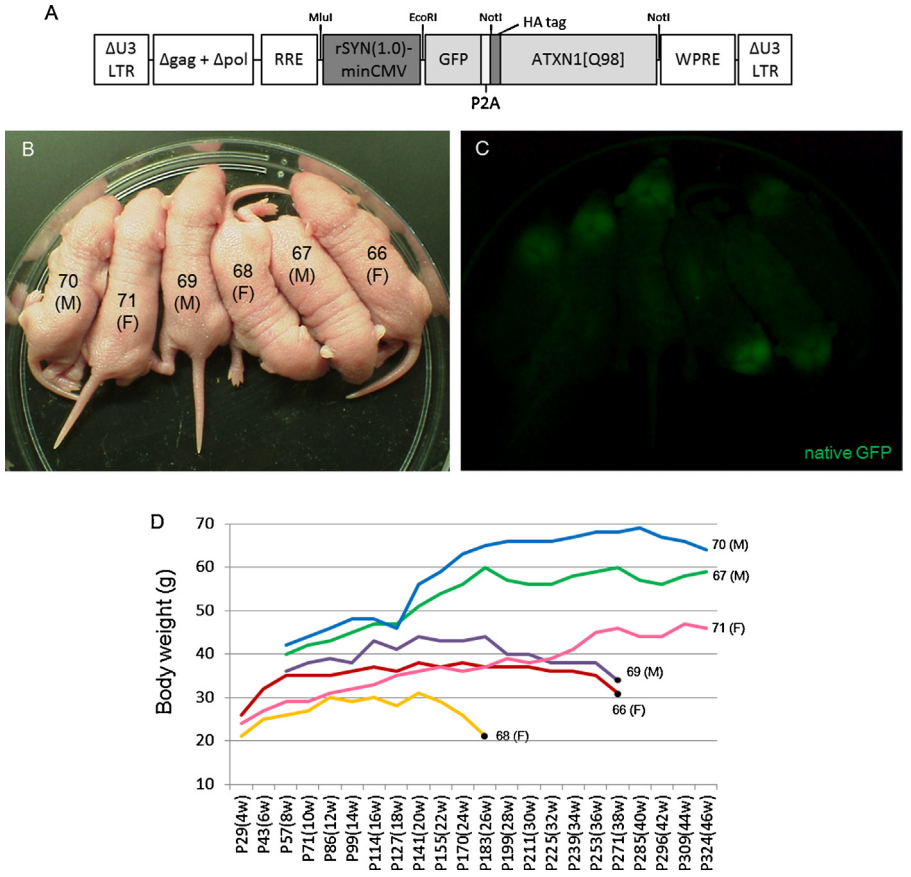

Fig. 4. Lentiviral-generated transgenic mice expressing GFP and ATXN1 with an abnormally expanded polyglutamine stretch. (A) A diagram depicting the provirus flanked by ΔU3LTRs. Transcription of GFP and an ataxin-1 cDNA containing 98 CAG repeats (ATXN1[Q98]) driven by rSynI(1.0)-minCMV. A human influenza hemagglutinin (HA) tag was attached to the 5′ end of ATXN1[Q98]. A self-cleaving 2A sequence (P2A) was inserted between GFP and mutant ataxin-1 cDNA to express ATXN1[Q98] freed from GFP. (B and C) Bright field (B) and GFP fluorescent (C) stereoscopic images of the transgenic pups. The number and sex (male or female) of each mouse is indicated on the body. (D) A graph showing changes in the body weights of transgenic mice. Because transgenic mice no. 68, no. 69 and no. 66 developed severe ataxia with decreased body weight, the animals were sacrificed to examine the pathological changes in the brain at the points indicated with black dots.

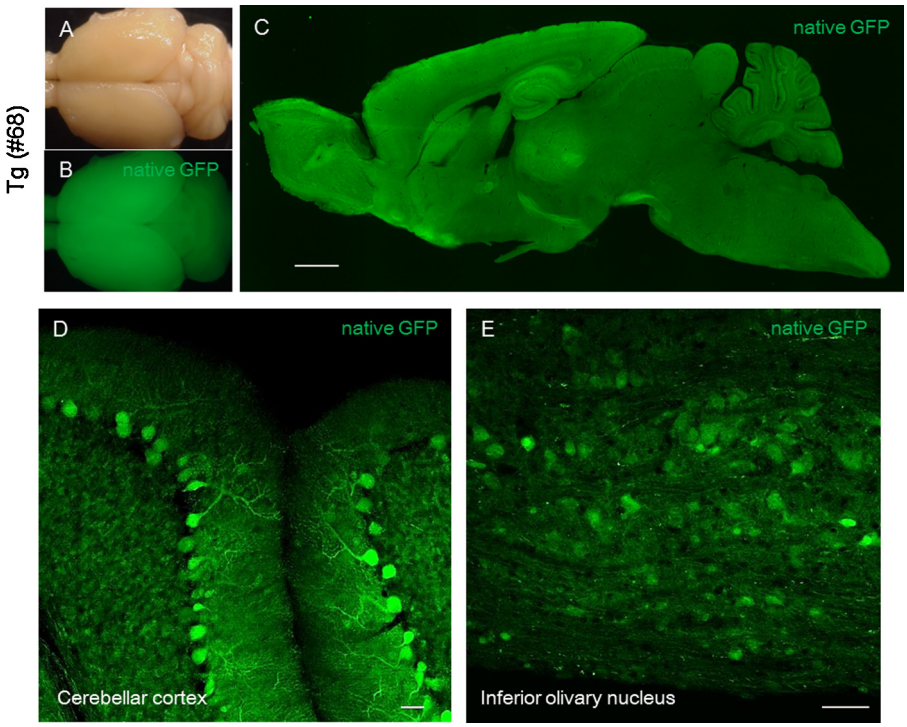

Fig. 5. Native GFP in the brain of a transgenic mouse (no. 68, P185) expressing GFP and ATXN1[Q98]. The transgenic mouse (no. 68) did not gain weight until 12 weeks after birth and began to lose weight at 20 weeks after birth. In parallel, a progression toward severe ataxia was noted among the littermates. The mouse was sacrificed at P185 for pathological examination. (A and B) Bright field (A) and GFP fluorescent (B) stereoscopic images of the whole brain of the transgenic mouse. (C) A sagittal section of the brain. Note that GFP was expressed throughout the transgenic brain, similar to the pattern observed in transgenic mice expressing GFP alone. (D and E) Enlarged images of the regions primarily affected by SCA1, including the cerebellar cortex (D) and the inferior olivary nucleus (E). Scale bars = 1 mm (C), 20 μm (D) and 50 μm (E).

nuclei, pontine nuclei, hippocampus and cerebral cortex (Fig. 6). These aggregates were not observed in the control wild-type mice (Fig. 6P–T). In the cerebellar cortex, strong immunoreactivity was observed in Purkinje cell nuclei (Fig. 6A, F and K). The thickness of the molecular layer was significantly decreased in SCA1 model mice compared with the control wild-type mouse (arrows indicate the top and bottom of the layer, Fig. 6A, F, K and P) (Fig. 7). In the deep cerebellar nuclei, immunoreactivity was primarily observed in large glutamatergic neurons. Thus, although the expression of the transgene differed among the transgenic individuals, the transgene was stably expressed throughout the brain, indicating the reliability and stability of rSynI(1.0)-minCMV for diffuse transgene expression in neurons of the CNS.

4. Discussion

In this study, we generated a mouse model of a neurodegenerative disease, SCA1, using lentiviral vectors containing a 1.0-kb rat SynI promoter fused with minCMV at the 3′ end. Transgenic mice expressed mutant ataxin-1 specifically in neurons throughout the CNS. A detailed examination using immunohistochemistry revealed nuclear aggregates of mutant ataxin-1 in the primary regions affected by SCA1, including the cerebral cortex, cerebellar cortex, deep cerebellar nuclei and brainstem (Seidel et al., 2012).

Various neuron-specific transgenic mice have been produced for studying molecules of unknown function and for examining the pathology of and developing novel therapies for neuronal diseases (Boy et al., 2010; Burright et al., 1995; Gendron and Petrucelli, 2011; Nuber et al., 2008; Torashima et al., 2008; Wen et al., 2002). Although transgenic mice expressing transgenes driven by the SynI promoter have been generated (Hoesche et al., 1993), its weak transcriptional activity, which is a common feature of cell type-specific promoters, often yields ambiguous outcomes. To avoid ambiguity, a tetracycline-controlled transactivation system (Gossen and Bujard, 1992; Odeh et al., 2011) has been used to compensate for the insufficient transcriptional activity of the SynI promoter (Chen et al., 2013; Kuhn et al., 2012; Sargeant et al., 2012). However, a several studies have demonstrated the toxicity of the tetracycline transactivator (McCloskey et al., 2005; Morimoto and Kopan, 2009; Sisson et al., 2006), which sometimes influences the phenotypes of the resultant transgenic rodents, including their behavior (Barton et al., 2002; Han et al., 2012). Using lentiviral vector-mediated transgene expression in the mouse brain *in vivo*, a recent study demonstrated that the addition of the CMV enhancer to the SynI promoter strengthened promoter activity (Hioki et al., 2007). Thus, the viral vector-mediated expression system is a powerful approach for screening various promoter constructs. However, the transgene expression profile of a promoter in transgenic animals does not always correspond to that observed in viral vector-mediated expression (Oue et al., 2012), as promoter constructs inserted into the chromosome of transgenic mice might undergo various developmental modifications, such as DNA methylation and acetylation, thereby silencing or enhancing the promoter activity depending on the specific area and cell type. Therefore, after screening a promoter construct through viral vector-mediated expression in the brain *in vivo*, the transgene expression profile of the promoter should be further examined in transgenic mice.

The most commonly accepted method for the generation of transgenic mice is pronuclear injection of linearized DNA into fertilized oocytes (Gordon et al., 1980). A major disadvantage of this method is the relatively low efficiency, particularly in species other than mice (Hirabayashi et al., 2001; Park, 2007). Although disease models of non-human primates are crucial for the clinical translation of results from basic research, there is a significant

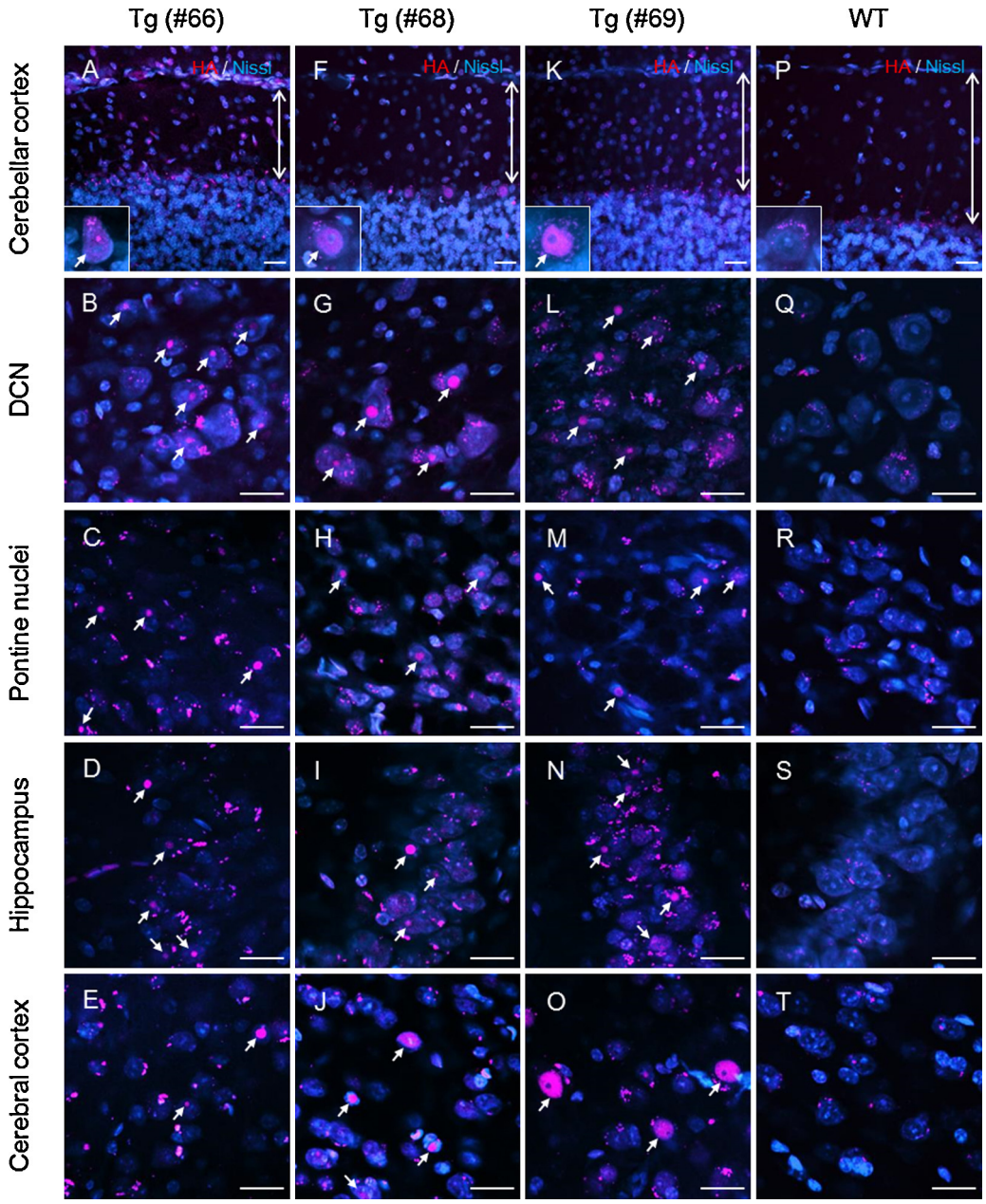

Fig. 6. ATXN1[Q98] aggregates in neurons of various regions primarily affected by SCA1. Sagittal sections from the transgenic mice expressing GFP and ATXN1[Q98] (no. 66, no. 68 and no. 69) and the control wild-type mouse were double-immunostained for Nissl substance (blue) and HA (magenta) fused to the amino-terminus of ATXN1[Q98]. Diffuse cytoplasmic granular spots immunolabeled with the anti-HA antibody showed non-specific immunolabeling for lipofuscin, which accumulates in postmitotic cells with increasing age. (A, F, K and P) Cerebellar cortex; (B, G, L and Q) deep cerebellar nuclei (DCN); (C, H, M and R) pontine nuclei; (D, I, N and S) hippocampus; (E, J, O and T) cerebral cortex. ATXN1[Q98] was localized specifically in the neurons in the brain areas examined. Note that the thickness of the molecular layer, indicated with the vertical arrows, is markedly thinner in transgenic mice expressing ATXN1[Q98] and GFP (A, F and K) compared with the control wild-type mouse (P). Scale bar = 20 μm. (For interpretation of the references to color in this figure legend, the reader is referred to the web version of this article.)

obstacle to the generation of transgenic non-human primates using conventional methods. The lentiviral vector-mediated insertion of a transgene into the chromosome is another approach for the generation of transgenic animals (Oue et al., 2012; Park, 2007). Indeed, transgenic marmosets expressing GFP under the control of constitutive viral promoters have previously been developed (Sasaki et al., 2009). Lentiviral transgenesis has several advantages over conventional pronuclear injection, which includes the production of transgenic animals with higher efficiency, particularly in species other than mice (Park, 2007). Moreover, the low transcriptional activity of cell type-specific promoters can be boosted through the addition of the WPRE downstream of the gene of interest. For the lentiviral transfer of a transgene, the size of the transgene flanked by the long terminal repeats should be less than 8 kb because of packaging limitations; if the transgene size is within these limits, it can be efficiently expressed. In this study, we used a 1.0-kb rat SynI promoter, which showed increased transcriptional activity without compromised neuronal specificity when a 128-bp minCMV sequence was fused to its 3′ end. Approximately 14 of the 19 animals born during this study possessed transgenes, and most of the animals robustly expressed the transgene throughout the CNS. The discrepancy between our results and those of previous reports showing absent or faint transgene expression in the cerebellum or brainstem (Nakagawa et al., 2006; Sargeant et al., 2012) might reflect the use of a longer SynI promoter. Alternatively, the appended minCMV might have strengthened the SynI promoter

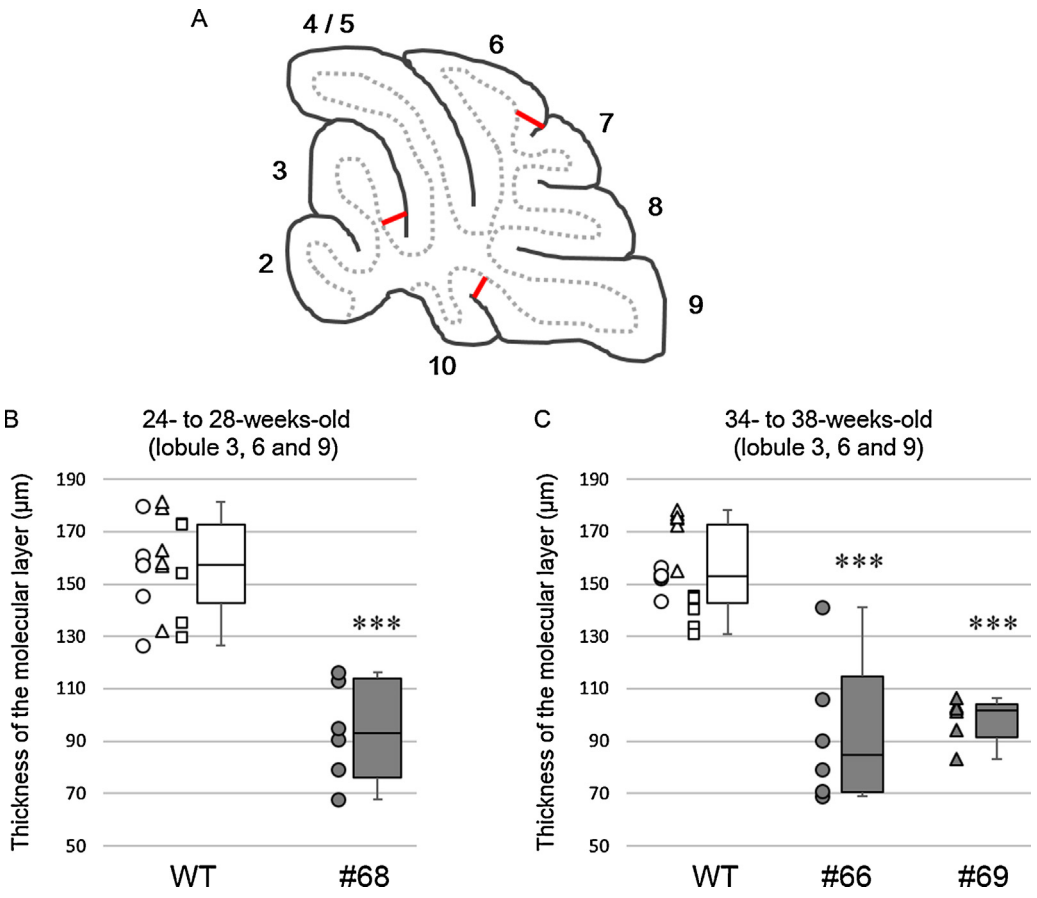

Fig. 7. Decrease in the thickness of the molecular layers in SCA1 model mice. (A) Schema depicting the locations at which the thickness of the molecular layer was measured. (B and C) Molecular layer thickness of SCA1 model mice no. 68 (26 weeks old), no. 66 and no. 69 (both 38 weeks old) and age-matched wild-type mice (WT). The molecular layer thickness was measured at three lobules using two cerebellar slices per mouse. Circles, triangles and squares are values obtained from different animals. For each box, the box boundaries indicate the first and third quartiles, the middle lines in the boxes indicate the median and the whiskers represent the lowest and highest values. Asterisks above the whiskers indicate significant differences between the wild-type and SCA1 model mice as determined by the Wilcoxon–Mann–Whitney test ($^{***}p < 0.001$).

activity sufficiently such that the transgene was also expressed in the hindbrain.

The transgenic mice expressing mutant ataxin-1 displayed ataxic behavior. Immunohistochemistry revealed mutant protein aggregates consistently in the nuclei of neurons in the major brain regions affected by SCA1. Thus, the 1.0-kb rat SynI promoter attached to minCMV exhibited great potential for the stable and robust expression of a transgene throughout the CNS. Because the SynI promoter is highly homologous across species, a transgene expression profile similar to that observed in this study might be obtained using the same SynI promoter in different animals, including non-human primates. Therefore, lentiviral transgenesis using this modified SynI promoter may be employed in the generation of various animal models, including non-human primates, for diseases that affect the CNS, such as several major types of SCA.

Conflict of interest statement

These authors declare no actual or potential conflicts of interest concerning the work presented in this manuscript.

Acknowledgments

This work was supported by a grant from the Funding Program for Next Generation World-Leading Researchers (LS021) (to H. Hirai).

Appendix A. Supplementary data

Supplementary data associated with this article can be found, in the online version, at http://dx.doi.org/10.1016/j.jneumeth.2013.12.004.

References

Barton MD, Dunlop JW, Psaltis G, Kulik J, DeGennaro L, Kwak SP. Modified GFAP promoter auto-regulates tet-activator expression for increased transactivation and reduced tTA-associated toxicity. Brain Research Molecular Brain Research 2002;101:71–81.

Boulos S, Meloni BP, Arthur PG, Bojarski C, Knuckey NW. Assessment of CMV, RSV and SYN1 promoters and the woodchuck post-transcriptional regulatory element in adenovirus vectors for transgene expression in cortical neuronal cultures. Brain Research 2006;1102:27–38.

Boy J, Schmidt T, Schumann U, Grasshoff U, Unser S, Holzmann C, Schmitt I, Karl T, Laccone F, Wolburg H, Ibrahim S, Riess O. A transgenic mouse model of spinocerebellar ataxia type 3 resembling late disease onset and gender-specific instability of CAG repeats. Neurobiology of Disease 2010;37:284–93.

Brunk UT, Terman A. Lipofuscin: mechanisms of age-related accumulation and influence on cell function. Free Radical Biology and Medicine 2002;33:611–9.

Burright EN, Clark HB, Servadio A, Matilla T, Feddersen RM, Yunis WS, Duvick LA, Zoghbi HY, Orr HT. SCA1 transgenic mice: a model for neurodegeneration caused by an expanded CAG trinucleotide repeat. Cell 1995;82:937–48.

Chen Y, Cao L, Luo C, Ditzel DA, Peter J, Sprengel R. Gene transfer of reversibly controlled polycistronic genes. Molecular Therapy Nucleic Acids 2013;2:e85.

Dittgen T, Nimmerjahn A, Komai S, Licznerski P, Waters J, Margrie TW, Helmchen F, Denk W, Brecht M, Osten P. Lentivirus-based genetic manipulations of cortical neurons and their optical and electrophysiological monitoring in vivo. Proceedings of the National Academy of Sciences of the United States of America 2004;101:18206–11.

Donello JE, Loeb JE, Hope TJ. Woodchuck hepatitis virus contains a tripartite post-transcriptional regulatory element. Journal of Virology 1998;72:5085–92.

Donnelly ML, Luke G, Mehrotra A, Li X, Hughes LE, Gani D, Ryan MD. Analysis of the aphthovirus 2A/2B polyprotein 'cleavage' mechanism indicates not a proteolytic reaction, but a novel translational effect: a putative ribosomal 'skip'. The Journal of General Virology 2001;82:1013–25.

Gendron TF, Petrucelli L. Rodent models of TDP-43 proteinopathy: investigating the mechanisms of TDP-43-mediated neurodegeneration. Journal of Molecular Neuroscience 2011;45:486–99.

Gordon JW, Scangos GA, Plotkin DJ, Barbosa JA, Ruddle FH. Genetic transformation of mouse embryos by microinjection of purified DNA. Proceedings of the National Academy of Sciences of the United States of America 1980;77:7380–4.

Gossen M, Bujard H. Tight control of gene expression in mammalian cells by tetracycline-responsive promoters. Proceedings of the National Academy of Sciences of the United States of America 1992;89:5547–51.

Guo JT, Yu J, Grass D, de Beer FC, Kindy MS. Inflammation-dependent cerebral deposition of serum amyloid a protein in a mouse model of amyloidosis. The Journal of Neuroscience: The Official Journal of the Society for Neuroscience 2002;22:5900–9.

Han HJ, Allen CC, Buchovecky CM, Yetman MJ, Born HA, Marin MA, Rodgers SP, Song BJ, Lu HC, Justice MJ, Probst FJ, Jankowsky JL. Strain background influences neurotoxicity and behavioral abnormalities in mice expressing the tetracycline transactivator. The Journal of Neuroscience: The Official Journal of the Society for Neuroscience 2012;32:10574–86.

Heumann R, Goemans C, Bartsch D, Lingenhohl K, Waldmeier PC, Hengerer B, Allegrini PR, Schellander K, Wagner EF, Arendt T, Kamdem RH, Obst-Pernberg K, Narz F, Wahle P, Berns H. Transgenic activation of Ras in neurons promotes hypertrophy and protects from lesion-induced degeneration. The Journal of Cell Biology 2000;151:1537–48.

Hioki H, Kameda H, Nakamura H, Okunomiya T, Ohira K, Nakamura K, Kuroda M, Furuta T, Kaneko T. Efficient gene transduction of neurons by lentivirus with enhanced neuron-specific promoters. Gene Therapy 2007;14:872–82.

Hirabayashi M, Takahashi R, Ito K, Kashiwazaki N, Hirao M, Hirasawa K, Hochi S, Ueda M. A comparative study on the integration of exogenous DNA into mouse, rat, rabbit, and pig genomes. Experimental Animals 2001;50:125–31.

Hoesche C, Sauerwald A, Veh RW, Krippl B, Kilimann MW. The 5′-flanking region of the rat synapsin I gene directs neuron-specific and developmentally regulated reporter gene expression in transgenic mice. The Journal of Biological Chemistry 1993;268:26494–502.

Holzer M, Gartner U, Klinz FJ, Narz F, Heumann R, Arendt T. Activation of mitogen-activated protein kinase cascade and phosphorylation of cytoskeletal proteins after neurone-specific activation of p21ras I. Mitogen-activated protein kinase cascade. Neuroscience 2001;105:1031–40.

Iizuka A, Takayama K, Torashima T, Yamasaki M, Koyama C, Mitsumura K, Watanabe M, Hirai H. Lentiviral vector-mediated rescue of motor behavior in spontaneously occurring hereditary ataxic mice. Neurobiology of Disease 2009;35:457–65.

Ingram MA, Orr HT, Clark HB. Genetically engineered mouse models of the trinucleotide-repeat spinocerebellar ataxias. Brain Research Bulletin 2012;88:33–42.

Kugler S, Kilic E, Bahr M. Human synapsin 1 gene promoter confers highly neuron-specific long-term transgene expression from an adenoviral vector in the adult rat brain depending on the transduced area. Gene Therapy 2003;10:337–47.

Kuhn B, Ozden I, Lampi Y, Hasan MT, Wang SS. An amplified promoter system for targeted expression of calcium indicator proteins in the cerebellar cortex. Frontiers in Neural Circuits 2012;6:49.

Kuzmich AI, Vvedenskii AV, Kopantzev EP, Vinogradova TV. Quantitative comparison of gene co-expression in a bicistronic vector harboring IRES or coding sequence of porcine teschovirus 2A peptide. Russian Journal of Bioorganic Chemistry 2013;39:406–16.

Laccone F, Maiwald R, Bingemann S. A fast polymerase chain reaction-mediated strategy for introducing repeat expansions into CAG-repeat containing genes. Human Mutation 1999;13:497–502.

McCloskey DT, Turnbull L, Swigart PM, Zambon AC, Turcato S, Joho S, Grossman W, Conklin BR, Simpson PC, Baker AJ. Cardiac transgenesis with the tetracycline transactivator changes myocardial function and gene expression. Physiological Genomics 2005;22:118–26.

Morimoto M, Kopan R. rtTA toxicity limits the usefulness of the SP-C-rtTA transgenic mouse. Developmental Biology 2009;325:171–8.

Morimoto S, Cassell MD, Sigmund CD. Neuron-specific expression of human angiotensinogen in brain causes increased salt appetite. Physiological Genomics 2002;9:113–20.

Nakagawa T, Feliu-Mojer MI, Wulf P, Lois C, Sheng M, Hoogenraad CC. Generation of lentiviral transgenic rats expressing glutamate receptor interacting protein 1 (GRIP1) in brain, spinal cord and testis. Journal of Neuroscience Methods 2006;152:1–9.

Nandy K. Properties of neuronal lipofuscin pigment in mice. Acta Neuropathologica 1971;19:25–32.

Nuber S, Petrasch-Parwez E, Winner B, Winkler J, von Horsten S, Schmidt T, Boy J, Kuhn M, Nguyen HP, Teismann P, Schulz JB, Neumann M, Pichler BJ, Reischl G, Holzmann C, Schmitt I, Bornemann A, Kuhn W, Zimmermann F, Servadio A, Riess O. Neurodegeneration and motor dysfunction in a conditional model of Parkinson's disease. The Journal of Neuroscience: The Official Journal of the Society for Neuroscience 2008;28:2471–84.

Odeh F, Leergaard TB, Boy J, Schmidt T, Riess O, Bjaalie JG. Atlas of transgenic Tet-Off Ca^{2+}/calmodulin-dependent protein kinase II and prion protein promoter activity in the mouse brain. NeuroImage 2011;54:2603–11.

Orr HT, Chung MY, Banfi S, Kwiatkowski TJ Jr, Servadio A, Beaudet AL, McCall AE, Duvick LA, Ranum LP, Zoghbi HY. Expansion of an unstable trinucleotide CAG repeat in spinocerebellar ataxia type 1. Nature Genetics 1993;4:221–6.

Oue M, Handa H, Matsuzaki Y, Suzue K, Murakami H, Hirai H. The murine stem cell virus promoter drives correlated transgene expression in the leukocytes and cerebellar Purkinje cells of transgenic mice. PloS One 2012;7:e51015.

Park F. Lentiviral vectors: are they the future of animal transgenesis. Physiological Genomics 2007;31:159–73.

Sargeant TJ, Drage DJ, Wang S, Apostolakis AA, Cox TM, Cachon-Gonzalez MB. Characterization of inducible models of Tay-Sachs and related disease. PLoS Genetics 2012;8:e1002943.

Sasaki E, Suemizu H, Shimada A, Hanazawa K, Oiwa R, Kamioka M, Tomioka I, Sotomaru Y, Hirakawa R, Eto T, Shiozawa S, Maeda T, Ito M, Ito R, Kito C, Yagihashi C, Kawai K, Miyoshi H, Tanioka Y, Tamaoki N, Habu S, Okano H, Nomura T. Generation of transgenic non-human primates with germline transmission. Nature 2009;459:523–7.

Scott BB, Lois C. Generation of tissue-specific transgenic birds with lentiviral vectors. Proceedings of the National Academy of Sciences of the United States of America 2005;102:16443–7.

Seidel K, Siswanto S, Brunt ER, den Dunnen W, Korf HW, Rub U. Brain pathology of spinocerebellar ataxias. Acta Neuropathologica 2012;124:1–21.

Sisson TH, Hansen JM, Shah M, Hanson KE, Du M, Ling T, Simon RH, Christensen PJ. Expression of the reverse tetracycline-transactivator gene causes emphysema-like changes in mice. American Journal of Respiratory Cell and Molecular Biology 2006;34:552–60.

Torashima T, Koyama C, Iizuka A, Mitsumura K, Takayama K, Yanagi S, Oue M, Yamaguchi H, Hirai H. Lentivector-mediated rescue from cerebellar ataxia in a mouse model of spinocerebellar ataxia. EMBO Reports 2008;9:393–9.

Torashima T, Okoyama S, Nishizaki T, Hirai H. In vivo transduction of murine cerebellar Purkinje cells by HIV-derived lentiviral vectors. Brain Research 2006;1082:11–22.

Wen PH, Shao X, Shao Z, Hof PR, Wisniewski T, Kelley K, Friedrich VL Jr, Ho L, Pasinetti GM, Shioi J, Robakis NK, Elder GA. Overexpression of wild type but not an FAD mutant presenilin-1 promotes neurogenesis in the hippocampus of adult mice. Neurobiology of Disease 2002;10:8–19.

Zufferey R, Donello JE, Trono D, Hope TJ. Woodchuck hepatitis virus posttranscriptional regulatory element enhances expression of transgenes delivered by retroviral vectors. Journal of Virology 1999;73:2886–92.